Fragmentation of ^{16}O and ^{18}O projectiles

S. L. Tabor, L. C. Dennis, K. W. Kemper, J. D. Fox, K. Abdo,* and G. Neuschaefer

Department of Physics, Florida State University, Tallahassee, Florida 32306

D. G. Kovar and H. Ernst

Physics Division, Argonne National Laboratory, Argonne, Illinois 60439

(Received 24 March 1981)

The energy spectra of particles lighter than the beam have been measured following the bombardment of ^{12}C, ^{27}Al, and ^{46}Ti targets with 72 MeV ^{16}O beams and 72 and 141 MeV ^{18}O beams. All the spectra exhibit broad continuum peaks centered at approximately the beam velocity. The shapes of these continuum structures are rather well reproduced by a fragmentation model which assumes that the unobserved fragment is transferred to the target and which contains no adjustable parameters. The ^{18}O fragmentation spectra on the three targets are very similar in shape. The total yield of fragmentation products is about the same for the ^{16}O and ^{18}O beams at 72 MeV, although the Z distribution of strength differs. On the other hand, the fragmentation yield of ^{18}O increases by a factor of 5 when the beam energy is raised from 72 to 141 MeV, but the relative Z distribution of strength remains constant.

$$\left[\begin{array}{l} \text{NUCLEAR REACTIONS } ^{12}\text{C, } ^{27}\text{Al, } ^{46}\text{Ti}(^{16}\text{O},X) \text{ and } (^{18}\text{O},X), X = \text{Li,} \\ \text{Be, B, C, N, } E = 72 \text{ and } 141 \text{ MeV; measured } d\sigma/d\Omega(E,\theta). \end{array} \right]$$

I. INTRODUCTION

For many projectiles, the spectra of particles lighter than the beam is dominated by broad peaks centered near energies corresponding to the beam velocity.[1−8] The systematics suggest that the observed particles are fragments of the projectile with only a spectator role in the reaction. The fragmentation process is an important one to be studied because it accounts for a significant fraction of the total reaction cross section.

Various forms of a simple semiclassical projectile fragmentation model provide a fairly reasonable description[1−4,9,10] of the measured data. In this model the observed spectra result from the momentum distributions of the fragments in the projectile after transformation from a coordinate system moving with the projectile into the laboratory system and multiplication by a phase-space factor. More detailed calculations have also been made using the distorted-wave Born approximation.[11−15] There is general agreement that the dominant process is one in which the unobserved fragment is transferred to the target.[3,4,9−11,14−16] However, there is considerably less agreement on the semantic question.

Names such as "projectile fragmentation," "massive transfer," "stripping to the continuum," and "incomplete fusion" appear to be used for the same process.

We undertook this investigation of ^{16}O and ^{18}O fragmentation partly to examine the roles of projectile, target, and incident energy in the reaction and partly to obtain more examples of the process to ascertain which features are systematic. Since simple fragmentation models predict that the spectral shapes are determined almost entirely by the properties of the projectile, it is important to examine their target dependence. It is also instructive to investigate the energy dependence of the fragmentation strength in the energy range in which the fusion cross section forms a decreasing fraction of the total reaction cross section.

II. EXPERIMENTAL PROCEDURE

Beams of 72 MeV ^{16}O and ^{18}O were provided by the Florida State University Super FN tandem accelerator. Self-supporting ^{27}Al targets of about 100 μg/cm^2 were used in an oil-free, cryo-pumped

scattering chamber to minimize carbon buildup. The reaction products were detected and identified with a gas ionization ΔE detector[17] and a Si surface barrier E detector.

The 141 MeV ^{18}O beam was provided by the tandem accelerator-superconducting linac system at Argonne National Laboratory. In this case, Si surface barrier detectors were used for both the ΔE and E detectors of the telescope. ^{12}C, ^{27}Al, and ^{48}Ti targets of 50, 100, and 150 $\mu g/cm^2$, respectively, were used.

The data were stored either in event mode on tape or in a large two-dimensional array to permit offline analysis. For both experiments, curved two-parameter gates were drawn in the ΔE-E plane around each Z group, and the data were projected onto a total energy axis for each Z group.
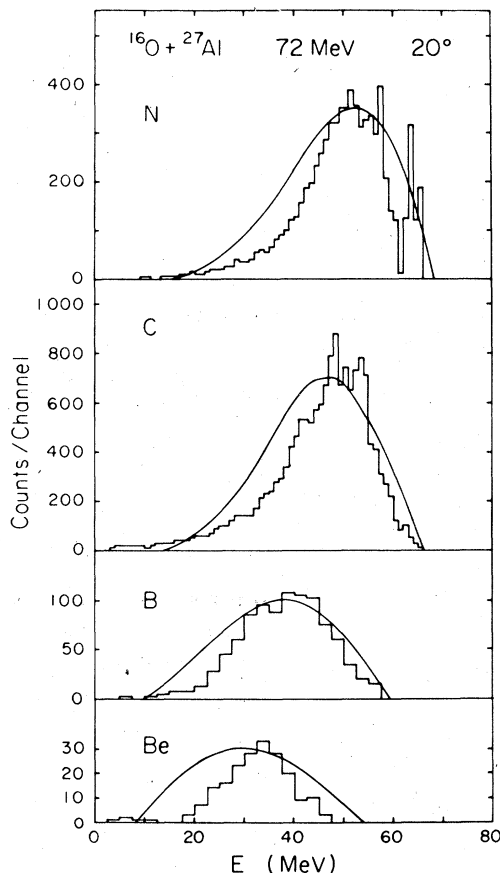

FIG. 1. The spectra of products of the ^{16}O + ^{27}Al reaction at $E_L = 72$ MeV and $\theta_L = 20°$ separated by element (Z) and plotted as a function of laboratory energy. The smooth curves are the results of a fragmentation model as discussed in the text.
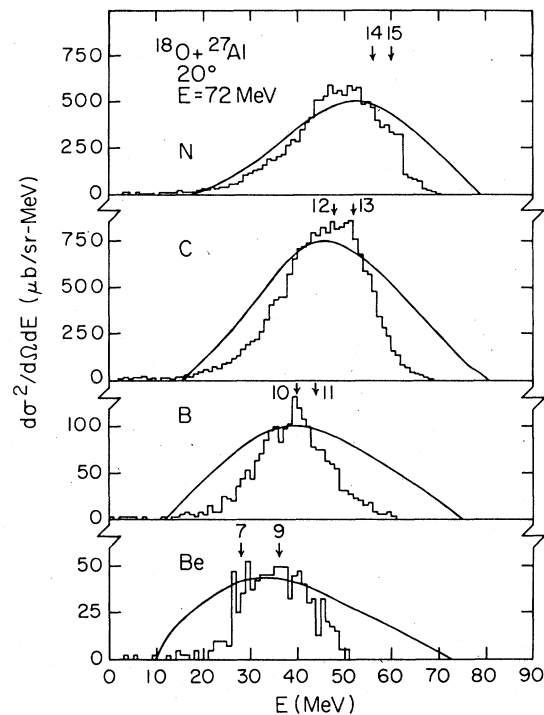

FIG. 2. The spectra of products of the ^{18}O + ^{27}Al reaction at $E_L = 72$ MeV and $\theta_L = 20°$ separated by element and plotted as a function of laboratory energy. The results of the fragmentation model discussed in the text are displayed as smooth curves.

III. RESULTS

Some typical spectra obtained in these experiments for particles lighter than the beam are shown in Figs. 1—4. They have been compressed by varying amounts to improve the statistical accuracy. The spectra are qualitatively similar to those seen for ^{14}N projectiles.[3] Some discrete lines can be seen in the spectra from the ^{16}O beam even after compression, but each spectrum is dominated by a broad continuum peak centered approximately at an energy corresponding to the beam velocity. Arrows are drawn in Figs. 2 and 3 to indicate the energy a particle of the labeled mass would have if traveling at the beam velocity. This is the zeroth order fragmentation model.

Since beam velocity particles may signal the occurrence of projectile fragmentation, we have compared the observed spectra with a simple breakup model.[2,3,9] The wave function of the fragments in the projectile is assumed to have a Yukawa shape
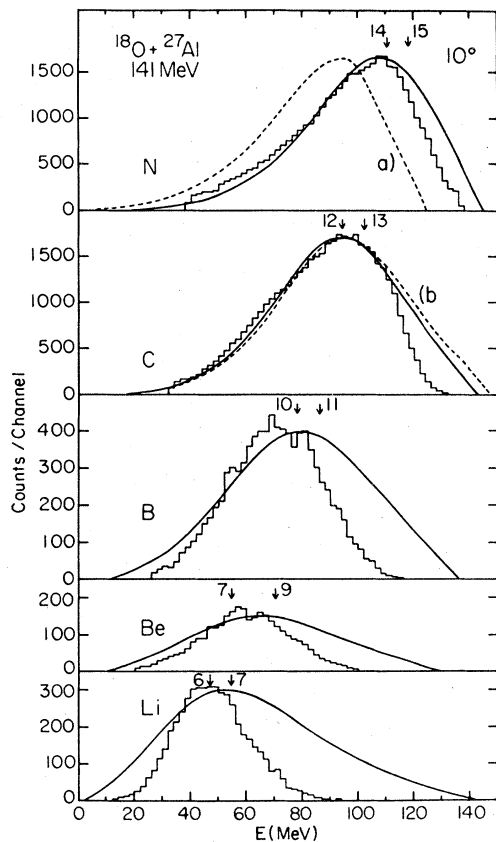
FIG. 3. The spectra of products of the ^{18}O + ^{27}Al reaction at $E_L = 141$ MeV and $\theta_L = 0°$ separated by element and plotted as a function of laboratory energy. The solid and dashed curves are model calculations discussed in the text.

FIG. 4. A comparison of the elemental spectra for the reactions ^{18}O + ^{12}C, ^{18}O + ^{27}Al, and ^{18}O + ^{48}Ti at $E_L = 141$ MeV and $\theta_L = 15°$. For each elemental product, the three curves have been normalized to equal areas.

whose size is determined by the binding energy. The fragment's resulting momentum distribution is added to its share of the beam's momentum to determine the energy spectrum. That spectrum is then multiplied by a phase space factor which approaches zero at the limits imposed by energy conservation. The local momenta at the point of interaction are corrected for the beam deceleration and fragment acceleration due to the Coulomb fields. The spectra for all the stable or long-lived isotopes of a given element calculated with this model are summed together and then arbitrarily normalized for comparison with the experimental elemental spectrum.

The dashed curve labeled "*a*" in the N spectrum of Fig. 3 represents a prediction of the fragmentation model assuming that both beam fragments remain free. The solid curve in that spectrum
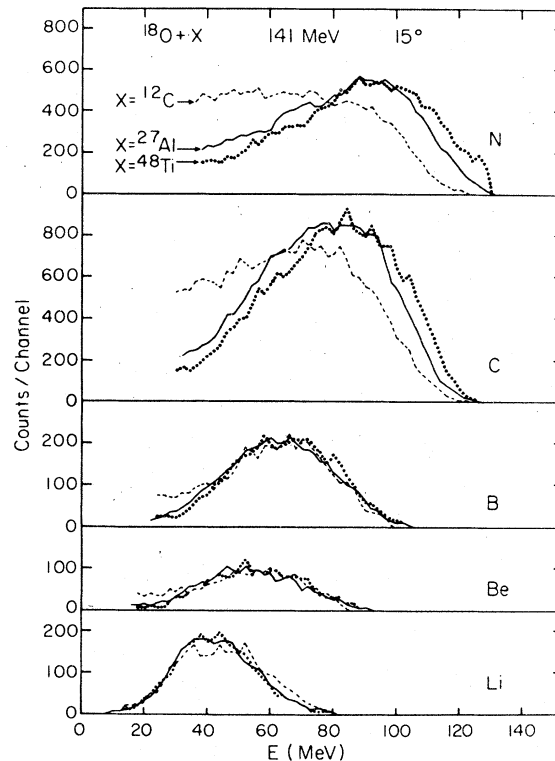
results from the same model under the assumption that the unobserved fragment fuses with the target. The major difference between these curves results from the difference in Q values for the two processes. Clearly, the data are better described by the hypothesis that the unobserved fragment is transferred to the target, although some small admixture of the other process is possible. A similar conclusion has been reached in a number of other fragmentation studies.[3,4,9–11,14,15] In particular, several coincidence measurements[16,18,19] have shown that the dominant fragmentation process leaves only two bodies in the final state. Hence, all the other curves are calculated assuming only two bodies in the final state.

The dashed curve labeled "*b*" in Fig. 3 shows the predictions of the fragmentation model exactly as it was formulated in Ref. 3. The solid curve in that spectrum and all the other smooth curves in Figs. 1 – 3 include an additional refinement, a fusion barrier between the unobserved fragment and the target
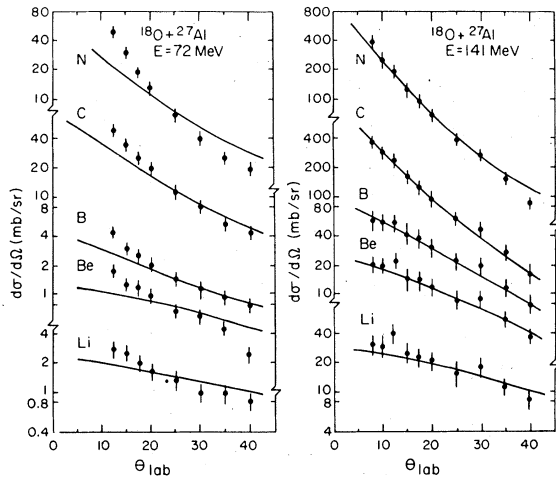
FIG. 5. Angular distributions of the products of the ¹⁸O + ²⁷Al reaction at 72 and 141 MeV separated by element. The results of the model discussed in the text are displayed as smooth curves.

been normalized so that there are equal areas under the curves for the three targets. The spectra generally look remarkably independent of target, another indication that the spectral shapes are determined largely by the velocity of and momentum distributions within the projectile. The target dependences of the high energy sides of the N and C spectra probably represent kinematic recoil effects. The low energy tails from the ¹²C target arise from evaporation residues following ¹⁸O + ¹²C fusion.

IV. DISCUSSION

The fragmentation model can also be compared with the measured angular distributions as shown in Fig. 5. The theoretical curves have been summed over the stable isotopes and then normalized for each Z group. It can be seen that the agreement in shape is quite good at 141 MeV. At 72 MeV the experimental angular distributions are somewhat
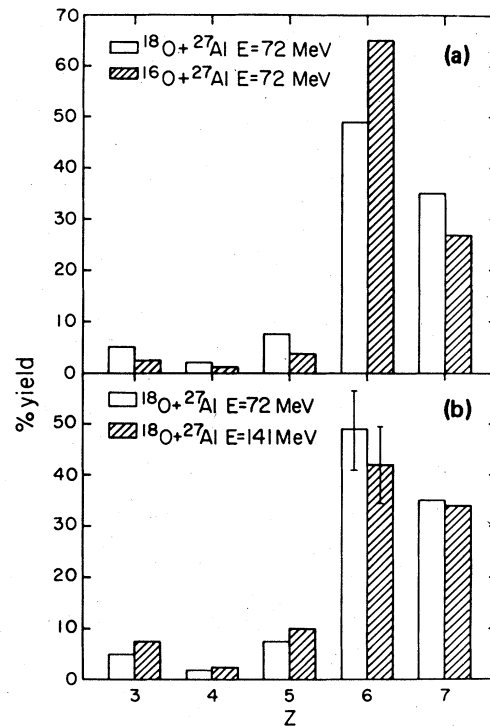
nucleus.[4] Although the effect of the fusion correction is not large, it has been included, since fragmentation-fusion appears to be the dominant process.

The fusion correction is based on the classical barrier formula,

$$\sigma_f = \pi r_B^2 (1 - V_B/E) ,$$

with

$$V_B = (Z_1 Z_2 e^2)/(r_B + 2.8 \text{ fm}) ,$$

and

$$r_B = 1.4(m_1^{1/3} + m_2^{1/3}) .$$

The constants were selected to reproduce the fusion systematics for light systems.[20]

It is clear from Figs. 1 — 3 that the fragmentation model reproduces the general behavior of the observed continuum peaks. There are no parameters in the model fitted to the data. The agreement is better for the heavier fragments, while the widths of the lighter fragment peaks are somewhat overestimated. Perhaps the binding energy prescription overestimates the fragment momentum distributions when the binding energy is large. The predicted spectra are closer in width to the measured ones for ¹⁴N projectiles[3] which are less tightly bound.

To investigate the target dependence, the ¹⁸O fragmentation spectra at 141 MeV are compared on targets of ¹²C, ²⁷Al, and ⁴⁸Ti in Fig. 4. The data have

FIG. 6. (a) A comparison of the relative distributins of the angle-integrated fragmentation cross sections as a function of atomic number Z for ¹⁶O and ¹⁸O projectiles at 72 MeV. (b) A similar comparison for ¹⁸O projectiles at 72 and 141 MeV.

steeper than the calculated ones. A comparison of Figs. 2 and 3 shows that the fragmentation model agrees somewhat better with the spectral shapes at the higher beam energy as well.

A comparison of the angle-integrated total fragmentation cross sections is also instructive. In the lower half of Fig. 6 the relative elemental yields for ^{18}O fragmentation are compared for beam energies of 72 and 141 MeV. The two distributions are relatively similar, with, perhaps, a slightly larger fraction of lighter fragments at the higher energy. The relative elemental yields for ^{16}O and ^{18}O fragmentation at 72 MeV are compared in the upper half of Fig. 6. The yield of C isotopes is greater for ^{16}O projectiles at the expense of all the other elements. This is presumably due to the significantly lower $^{12}C + \alpha$ breakup energy compared to the other channels.

Certain fragments have not been counted in this experiment. The yield of ^{16}O fragments is expected to be strong from the ^{18}O beam, but they were not adequately separated by the MZ^2 identification. The general trend in Fig. 6 is an even-odd effect modulating a declining yield with decreasing Z. The even-odd effect is presumably due to the more favorable Q values for even Z-even N fragments. If ^8Be had been detected, the Be yield would almost certainly have been larger than its neighbors. Finally, the light ions have not been included because of the problems of kinematically separating fragmentation and evaporation products and of possible double counting.

With these qualifications the total fragmentation cross sections for $3 \le Z \le Z_B - 1$ are compared in Fig. 7. A previous result for ^{14}N projectiles is included. The less tightly bound ^{14}N nucleus fragments more readily than ^{16}O or ^{18}O with 10 MeV more energy. Most spectacular is the five-fold increase in cross section for ^{18}O fragmentation when the beam energy is doubled. Even though they are lower limits for the total fragmentation yield, the values in Fig. 7 represent significant fractions of the total reaction cross section, especially at 141 MeV.

The rapid rise in the ^{18}O fragmentation yield occurs over an energy range in which the fusion cross section for comparable systems[20-22] has leveled off. Hence, the fragmentation process becomes an increasingly important competitor with the fusion process at beam energies above 100 MeV.
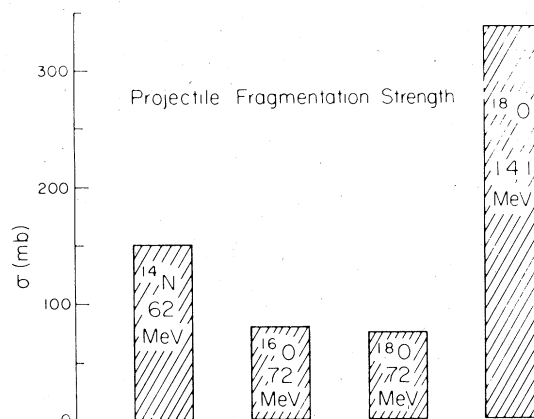

FIG. 7. A comparison of the total observed fragmentation cross sections for fragments with $3 \le Z < Z_{beam}$.

V. CONCLUSIONS

This work gives further evidence of the widespread occurrence of projectile fragmentation and of its importance in the overall picture of heavy-ion reactions. A simple parameter-free fragmentation model provides a reasonably good description of the spectral shapes and angular distributions of the particles lighter than the ^{16}O and ^{18}O beams. The agreement is better at the higher incident energy. The shapes of the ^{18}O fragmentation spectra are almost completely independent of target, confirming that they are determined largely by the projectile vertex in the reaction.

The ^{18}O fragmentation yield rises spectacularly with increasing beam energy. It increases five-fold to over 350 mb when the incident energy doubles. Hence, the fragmentation yield grows rapidly as an important part of the total reaction cross section while the fusion yields remains stagnant or falls. There is increasing evidence that fragmentation and fusion are the principal competitors in the heavy-ion reaction process.

*Permanent address: Department of Physics, Faculty of Science, University of Cairo, Giza, Egypt.

[1]J. R. Wu, C. C. Chang, and H. D. Holmgren, Phys. Lett. 40, 1013 (1978).

[2]N. Matsuoka, A. Shimizu, K. Hosono, T. Saito, M. Kondo, H. Sakaguchi, Y. Toba, A. Goto, F. Ohtani, and N. Nakanishi, Nucl. Phys. A311, 173 (1978).

[3]S. L. Tabor, L. C. Dennis, and K. Abdo,Phys. Rev. C (to be published).

[4]J. R. Wu and I. Y. Lee, Phys. Rev. Lett. 45, 8 (1980).

[5]H. Fröhlich, T. Shimoda, M. Ishihora, K. Nagatani, T. Udagawa, and T. Tamura, Phys. Rev. Lett. 42, 1518 (1979).

[6]C. M. Castaneda, H. A. Smith, Jr., P. P. Singh, and H. Karnowski, Phys. Rev. C 21, 179 (1980).

[7]C. K. Gelbke, C. Olmer, M. Buenerd, D. L. Hendrie, J. Mahoney, M. C. Mermaz, and D. K. Scott, Phys. Rep. 42C, 311 (1978).

[8]O. Bousshid, M. Machner, C. Alderliesten, U. Bechstedt, A. Djaloeis, P. Jahn, and C. Mayer-Böricke, Phys. Rev. Lett. 45, 980 (1980).

[9]R. Serber, Phys. Rev. 72, 1008 (1947).

[10]G. Baur, R. Shyam, F. Rösel, and D. Trautmann, Phys. Rev. C 21, 2668 (1980).

[11]T. Udagawa and T. Tamura, Phys. Rev. C 21, 1271 (1980).

[12]T. Udagawa, T. Tamura, and D. Price, Phys. Rev. C 21, 1891 (1980).

[13]T. Udagawa and T. Tamura, Phys. Rev. Lett. 45, 1311 (1980).

[14]H. Fröhlich, T. Shimoda, M. Ishihara, K. Nagatani, T. Udagawa, and T. Tamura, Phys. Rev. Lett. 42, 1518 (1979).

[15]R. Shyam, G. Baur, F. Rösel, and D. Trautmann, Phys. Rev. C 22, 1401 (1980).

[16]R. W. Koontz, C. C. Chang, H. D. Holmgren, and J. R. Wu, Phys. Rev. Lett. 43, 1862 (1979).

[17]M. M. Fowler and R. C. Jared, Nucl. Instrum. Methods 124, 341 (1975).

[18]E. Takada, T. Shimoda, N. Takahashi, T. Yamaya, K. Nagatani, T. Udagawa, and T. Tamura, Phys. Rev. C 23, 772 (1981).

[19]K. Siwek-Wilczynska, E. H. Du Marchie van Voorthuysen, J. Van Popta, R. H. Siemssen, and J. Wilczynski, Nucl. Phys. A330, 150 (1979).

[20]D. G. Kovar, D. F. Geesaman, T. H. Braid, Y. Eisen, W. Henning, T. R. Ophel, M. Paul, K. E. Rehm, S. J. Sanders, P. Sperr, J. P. Schiffer, S. L. Tabor, S. Vigdor, and B. Zeidman, Phys. Rev. C 20, 1305 (1979).

[21]S. L. Tabor, D. F. Geesaman, W. Henning, D. G. Kovar, K. E. Rehm, and F. W. Prosser, Jr., Phys. Rev. C 17, 2136 (1978).

[22]F. W. Prosser, Jr., R. A. Racca, K. Daneshvar, D. F. Geesaman, W. Henning, D. G. Kovar, K. E. Rehm, and S. L. Tabor, Phys. Rev. C 21, 1819 (1980).